Pulsed NMR Spin Echoes

Dennis V. Perepelitsa*
MIT Department of Physics
(Dated: March 10, 2007)

Pulsed nuclear magnetic resonance techniques with transverse radiofrequency pulses are used to determine the spin-lattice and spin-spin relaxation times of glycerol and Fe^{+++} solutions of varying concentrations. The nuclear magnetic moments of flourine and hydrogen are found to be $\mu_{H+} = (1.408 \pm .008) \times 10^{-26}$ J/T and $\mu_{F-} = (1.324 \pm .007) \times 10^{-26}$ J/T, respectively. A negative linear relation in log-log space is established between sample viscosity and paramagnetic ion concentration and relaxation with $\chi^2_\nu = 9.1$ and $\chi^2_\nu = 9.6$, respectively. Implications of Bloembergen's 1948 thesis are investigated.

1. INTRODUCTION

The technique of *nuclear magnetic resonance* (NMR) was developed simultaneously by F. Bloch [1] and E.M. Purcell in 1946 as a way of measuring the magnetic moment of a particle. In 1948, Bloembergen et. al. [2] catalogued *relaxation phenomena* that led to the decay of an observed signal. These relaxation times revealed interesting properties of the particle in solution and the magnetic field in which they were contained.

One finding of Bloembergen et. al. was that the *relaxation time* of some substances depended on the viscosity of the solution. For non-viscous solution, the concentration of paramagnetic ions seemed to play an analogous role. In both cases, the relationship was negative and linear in log-log space. Additionally, two different types of relaxation times for viscous liquids often had roughly the same values.

Two years later, in 1950, Hanh [3] discovered the *spin echo*, a phenomenon useful in recovering an otherwise lost part of an NMR signal. Later, in 1954, Carr and Purcell [4] would develop a method that eliminated the effects of undesirable diffusion effects while measuring relaxation time.

The measurement of the magnetic moment of the proton and the fluorine atom, as well as the relationship between relaxation times and varying viscosities and paramagnetic ion concentrations, are the prime purposes of this experiment.

2. THEORY

In the presence of an external magnetic field, particles with a nuclear magnetic moment will tend to line up in a direction parallel to the field. It is well known that if a particle with magnetic moment μ and spin I is displaced from the $\hat{z}$-direction in a field $B_0\hat{z}$, it will begin to *precess* around the field direction with what is called the *Larmor frequency*:

$$\omega = \frac{\mu B_0}{\hbar I} \tag{1}$$

We are interested in the projection of the particle's spin vector onto the perpendicular $\hat{x} - \hat{y}$-plane. Consider the ensemble of many such particles in a small region where the field is relatively homogeneous. Although their individual projections are quantized, Bloch [1] showed that the average spin of the system is described by a classical vector.

If a sample of particles is irradiated with a transverse oscillating radiofrequency (rf) pulse, the state vector begins to precess slowly around a vector *perpendicular* to that of the field, eventually passing through the $\hat{x} - \hat{y}$-plane. By careful timing of the rf pulses, an experimenter is able to manipulate the state vector.

Individual spin$-1/2$ particles are either in the spin-up or spin-down state. Since the former has a slightly lower energy configuration in a magnetic field, the Boltzmann distribution dictates that slightly more states are in the spin-up state. This inequality causes a slight net magnetization along the state vector. If the sample is placed in a solenoid, the changing magnetic flux caused by the precessing vector will induce a current. This is the mechanism through which we observe an NMR signal.

The rotation is a resonance phenomenon, and we require that the frequency of the rf-pulse closely match the Larmor frequency of the field. However, some interference is necessary, for it is the beat frequency between these two that accounts for the oscillating structure of the eventual output signals.

2.1. Relaxation Times and Pulse Sequences

Several different effects contribute to the eventual decoherence of the observed signal. The first of these is the *free induction decay* (FID) caused by the inhomogeneity of the magnetic field, which causes the individual precessing vectors to grow out of phase. In the literature, the other two are referred to as the *spin-lattice interaction* and the *spin-spin interaction*. We present methods to determine these experimentally.

*Electronic address: dvp@mit.edu

The *spin-lattice relaxation time* T_1 is a measure of how quickly the system "resets" back into the field-aligned low-energy configuration. If we rotate the system into the $x-y$-plane with a 90°-pulse, and wait for some small time while the system begins to recover, another 90° pulse will send the aligned projection of the state vector back into the perpendicular plane, where its signal can be measured. Thus, to measure the proportion of the signal recovered at a time τ, we measure the amplitude $A(\tau)$ of the second FID after two 90°-pulses separated by time τ. We expect an exponentially increasing relationship:

$$A(\tau) = C_1 - C_2 e^{-\tau/T_1} \tag{2}$$

The *spin-spin relaxation time* T_2 is a measure of how quickly transverse magnetization decays. When we rotate our system with a 90°-pulse, the induced signal quickly decoheres. However, if the sample experiences a 180°-pulse after some time, the phase difference between individual particles will be reversed, and the system will precess back into coherency after a similar period of time. We will see the spin echo described in [3], but some of the perpendicular magnetization will have decayed away. Thus, the amplitude of the spin echo $A(2\tau)$ after a $90° - 180°$-pulse sequence separated by time τ is given by

$$A(2\tau) = C_1 + C_2 e^{-2\tau/T_2} \tag{3}$$

An important detail is that since the particles in question do not feel the same magnetic field before and after the 180°-pulse, the decay will be a bit faster than exponential. Carr and Purcell [4] showed that the effects of field inhomogeneity may be ignored in the case of a 90°-pulse followed by successive 180°-pulses at evenly spaced intervals, if the intervals are of an order smaller than the relaxation time. It is therefore appropriate to expect that an application of the Carr-Purcell pulse sequence will result in the exponential decay given predicted in (3).

Since T_1 is a measure of how quickly the system returns to thermal equilibrium, and T_2 only concerns itself with the phase decoherence of *magnetized* particles, T_1 is necessarily an upper limit on T_2: a particle "cooled" into the z-direction cannot contribute to the magnetization of the system.

3. EXPERIMENTAL SETUP

The experimental setup used in our experiment is outlined with a block-diagram in Figure 1. The heart of the system is a programmable digital pulse programmer, which allows the experimenter to select microsecond-long pulse widths and choose their separation in milliseconds. This timing information is fed to a gate receiving a 10 dB sinusoidal signal from a function generator, with variable frequency. The rf signal is split, half of it amplified and sent to the sample, and half of it as a reference for the phase detector. At this point, a signal from the pulse generator also triggers the oscilloscope.

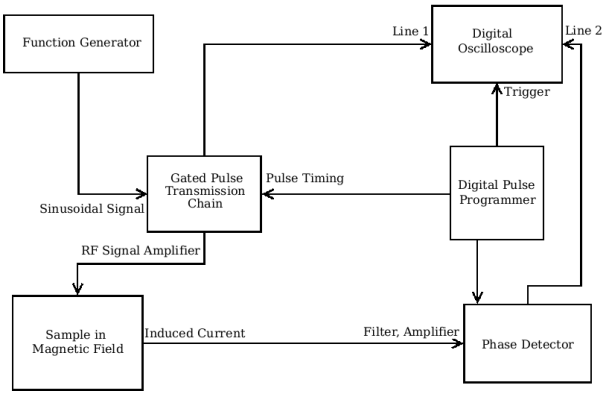

FIG. 1: Block diagram of experimental setup. Adapted from photography in [6].

The sample is suspended between two strong magnets inside a solenoid and is part of the *probe circuit*. The probe circuit consists of the sample in parallel with an adjustable capacitor for impedance matching, and this combination in series with a capacitor tuned to resonate with the frequency of the expected signal. The rf pulse enters the circuit, irradiates the sample, and the induced current is collected and leaves the probe circuit.

The weak signal is amplified and filtered, and enters the phase detector where it is compared with the reference signal of the generator. The resulting signal, which consists of "beats" arising from the slight frequency mismatch, is displayed on the oscilloscope. Since both the strong rf pulse and the weak response signal go through the same circuit, care must be taken to deal with both of them appropriately. In particular, a crossed pair of diodes between the end probe circuit and the sensitive pre-amplifier acts to ground any strong signal, and allows the weak signal to pass.

3.1. Methodology

We used a gaussmeter probe calibrated with a source of known strength accurate to ±.5% to determine the mean field strength in the area of the sample. We probed various spatial locations between the magnets, and calculated an rms inhomogeneity of ±4 Gauss.

We determined the Larmor frequency of hydrogen and fluorine ions in solution by varying the signal generator frequency and observing the size of the FID. Since the observed beat frequency is related to the difference between the Larmor frequency and the pulse frequency, we varied the latter until the observed waveform seemed to collapse.

We created Fe^{+++} ion solution samples with six values of paramagnetic ion concentration - 10^{15} to 10^{20} ions/cc, by starting with a concentrated sample and diluting ten-

fold several times. We then tuned the capacitor knob on the pulse circuit setup until any observed signal was at a maximum.

Next, to determine the length of an rf pulse that corresponded to a 180° rotation, we chose the first value of the pulse width that minimized the magnitude of the free induction decay. The length of a 90° pulse was taken to be half this. For proton NMR, we determined the length of these pulses to be 49 and 25 milliseconds, respectively, to the highest degree of accuracy allowed by the digital pulse programmer.

We determined the spin-lattice and the spin-spin relaxation time using the $90°-90°$ and Carr-Purcell sequences, respectively. In the former, we varied the time between pulses τ and measured the voltage of the highest beat within the decay envelope. In the latter, we did the same with the highest measured voltage that occurred during a spin echo. In both cases, we chose values of τ that allowed for twenty or so data points, which we later fit to a model function with numerical analysis techniques. We performed this routine for every ion concentration, concentrations of glycerin varying from 20% to 100% by weight, and nitrogen gas-bubbled water.

4. DATA ANALYSIS

Adding the calibration and inhomogeneity uncertainties in quadrature, the calculated field strength was

$$B_0 = 1772 \pm 10 \text{ Gauss} \tag{4}$$

There is error inherent in our method of measuring the height of FID and spin echo signals. Let T_{FID} be the decay constant of the exponentially decaying envelope, and P_{beat} be the period of an oscillations inside the envelope. We assume that the time of the first beat t is evenly distributed from 0 (right on the FID height) to P (an entire period away). The standard deviation is $\sigma_P = \frac{P}{\sqrt{12}}$, and error propagation leads to a relative uncertainty in our observed peak height:

$$A = A_0 e^{-t/T_{FID}} \Rightarrow \sigma_A = A_0 \frac{1}{T_{FID}} \sigma_t$$
$$\frac{\sigma_A}{A} = \frac{P}{T_{FID}\sqrt{12}} \tag{5}$$

In the case of the double-ended spin echo, the highest beat could only be off by up to half a period, and so we halve the relative uncertainty. In practice, the decay time of envelope was on the order of 400 microseconds, with a beat period of 30 microseconds, giving a relative uncertainty of approximately 3% in the case of an FID and 2% in the case of a spin echo.

Additionally, the technical specification of the oscilloscope [5] placed an upper bound of .06 mV on the resolution of our signal. We add this uncertainty with the one given in (5) in quadrature. Using this method to describe the uncertainty, we performed a least-squares non-linear fit of the $90° - 90°$ and Carr-Purcell data to (2) and (3), respectively. The resulting uncertainty in the fitted parameters T_1 and T_2 for each sample were a function of the relative uncertainties from other sources and the goodness of the fit.

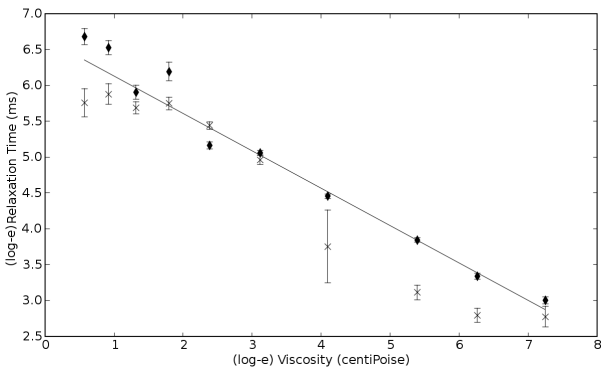

FIG. 2: Relaxation time versus viscosity. Logarithm of viscosity in centiPoise is on the abscissa, and the logarithm of the relaxation time in milliseconds is on the ordinate. The diamonds are spin-lattice times, and the crosses are spin-spin times.

In general, we were able to obtain good exponential fits to the observed data. Fits to the rising FID heights caused by $90° - 90°$ pulses had the majority of χ^2_ν values ranging from .5 to 1.5, with single-digit relative uncertainty in the calculated parameter value T_1. Fits to the decaying spin echo heights caused by the Carr-Purcell sequence were a little noisier: the majority of χ^2_ν values ranged from 1.0 to 2.0, with approximately 10% uncertainty in T_2.

4.1. Determination of the Magnetic Moment

With the method outlined above, we determined the Larmor precession frequency of the proton and fluorine atom to be $\omega = 7.5287 \pm .0002$ MHz and $\omega = 7.081 \pm .001$ MHz, respectively. Using the relation in (1) and the results in (4) we obtain

$$\mu_{H^+} = (1.408 \pm .008) \times 10^{-26} \text{ J/T}$$
$$\mu_{F^-} = (1.324 \pm .007) \times 10^{-26} \text{ J/T} \tag{6}$$

4.2. Viscosity Dependence

We were able to obtain a value for the spin-lattice and spin-spin relaxation time for a wide range of glycerin concentrations. Assuming that the temperature inside the room was $20°C$, we used the lab guide [6] to convert the concentration to a viscosity value.

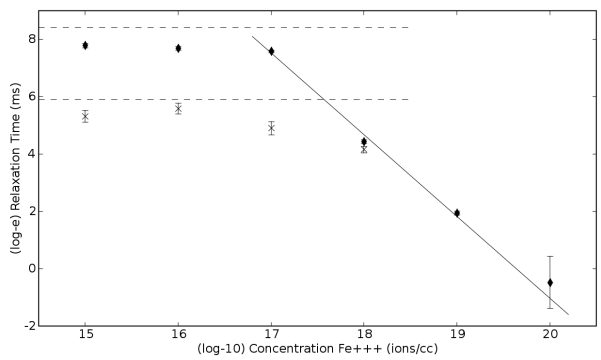

FIG. 3: Relaxation time versus paramagnetic ion concentration. Base-ten logarithm of concentration in ions per cubic centimeter is on the abscissa, and the logarithm of the relaxation time in milliseconds is on the ordinate. The diamonds are spin-lattice times, and the crosses are spin-spin times.

Following Bloembergen [2], Figure 2 shows the relationship between viscosity and spin-lattice relaxation time T_1 on a log-log scale for eleven values of the viscosity. The fitted line has slope $-.521 \pm .009$ with $\chi^2_\nu = 9.1$. The spin-spin relaxation times T_2 are plotted alongside those of T_1. As expected, they are roughly T_1, but always smaller.

4.3. Paramagnetic Ion Concentration Dependence

While we were able to obtain a measurement of T_1 for all six concentrations of iron solution, we were unable to obtain a measurement of T_2 for the 10^{19} ions/cc and 10^{20} ions/cc Fe^{+++} solutions. Figure 3 shows the relationship between paramagnetic ion concentration and both relaxation times. The higher and lower horizontal dotted lines are the spin-lattice and spin-spin relaxation times, respectively, of pure nitrogen-bubbled water. The fitted line shown has slope $-2.85 \pm .004$ with $\chi^2_\nu = 9.6$.

Two tendencies are salient. For high concentrations, the points seem to follow a line in log-log space. However, for sufficiently low concentrations, the relaxation times approach those of water and level off. This implies that at low concentrations, paramagnetic ions have relatively little impact on the relaxation time of the solution.

5. CONCLUSIONS

In general, our results are in good agreement with established findings. The derived values of the magnetic moments of hydrogen and fluorine were $(1.408 \pm .008) \times 10^{-26}$ J/T and $(1.324 \pm .007) \times 10^{-26}$ J/T, respectively. These are easily within one standard deviation of the NIST values $\mu_{H^+} = 1.411 \times 10^{-26}$ J/T and $\mu_{F^-} = 1.328 \times 10^{-26}$ J/T, respectively, and are accurate to within .3%.

We have established a negative linear relationship between the viscosity (or paramagnetic ion concentration) of a solution and spin-lattice relaxation time, with $\chi^2_\nu = 9.1$ (and $\chi^2_\nu = 9.6$, respectively). The unfortunately high chi parameter is probably an indicator that we are underestimating our error. Additionally, for low concentrations, we observed a "leveling off" of the relaxation time as it approached that of deoxygenated water. Lastly, in all but one case, T_1 was higher than T_2, as expected.

There were a few sources of random and systematic error that we did not consider in our model. We did not take into effect random fluctuations from background noise, modeling it as a constant offset instead. We have not modeled uncertainty in the concentration of Fe^{+++} ions or in that of glycerin. We have not considered the possibility that the appearance of the first beat within a decay envelope is systematic rather than random. All of these are areas for possible improvement in future experiments.

Our paper differs in several important ways from that of Bloembergen et. al. [2]. Though their results relating viscosity to relaxation time also showed a linear relation in log-log space, their coefficient was closer to $-\frac{2}{3}$, indicating a quantitatively different relationship. Furthermore, Bloembergen et. al. measured relaxation times for solutions with much higher concentrations of paramagnetic irons than the ones in this experiment. As such, they never observed the "cutoff" close to the relaxation time of water. This phenomenon is a strong candidate for further inquiry.

[1] F. Bloch, Phys. Rev. **70** (1946).
[2] R. P. N. Bloembergen, E.M. Purcell, Phys. Rev. **73** (1947).
[3] E. Hanh, Phys. Rev. **80** (1950).
[4] E. P. H.Y. Carr, Phys. Rev. **94** (1954).
[5] *Agilent oscilloscopes user's guide*, `http://cp.literature.agilent.com/litweb/pdf/54622-97036.pdf`.
[6] J. L. Staff, *Pulsed nuclear magnetic resonance: Spin echoes* (2006), jLab E-Library, URL `http://web.mit.edu/8.13/www/JLExperiments/JLExp12.pdf`.

Acknowledgments

DVP gratefully acknowledges Brian Pepper's equal partnership, as well as the guidance and advice of Thomas Walker, Daniel Nezich and Scott Sewell.